

BBAMEM 75850

## Calorimetric studies of fully hydrated phosphatidylcholines with highly asymmetric acyl chains

C. Huang, Z.-q. Wang, H.-n. Lin and E.E. Brumbaugh

*Department of Biochemistry, Health Sciences Center, University of Virginia, Charlottesville, VA (USA)*

(Received 14 August 1992)

**Key words:** Asymmetric mixed-chain phosphatidylcholine; Phosphatidylcholine; DSC; Mixed interdigitated bilayer; Phase transition behavior

We have semi-synthesized 52 molecular species of saturated diacyl mixed-chain phosphatidylcholines. All 52 phosphatidylcholine molecules are highly asymmetrical with  $\Delta C/CL$  values in the range of 0.43–0.63. The aqueous dispersions of these phosphatidylcholines have been studied by the high-resolution differential scanning calorimetric (DSC) technique. Upon heating, the lipid dispersions prepared individually from these 52 phosphatidylcholines all exhibit a sharp, single, endothermic peak at a characteristic temperature or  $T_m$ , implying that the self-assembled lipid molecules in excess water undergo the mixed interdigitated gel to the liquid-crystalline phase transition. The  $T_m$  values obtained from aqueous lipid dispersions prepared from these mixed-chain phospholipids have been analyzed based on the molecular packing model of the mixed interdigitated bilayer, and a linear relationship between the  $T_m$  and  $(\Delta C)^{-1}$  for various phospholipids at a constant value of  $\delta$  is observed. Based on these linear relationships, empirical equations are derived to predict the  $T_m$  values for highly asymmetrical mixed-chain phosphatidylcholines with  $\Delta C/CL$  values in the range of 0.43–0.63. The predictive power of these empirical equations is shown to be very good, since a comparison between the predicted and the experimental data indicates that the largest relative error in Kelvin is only 0.4%. A table containing 81 predicted  $T_m$  values for highly asymmetrical mixed-chain phosphatidylcholines is presented. The definitions of the various structural parameters such as  $\Delta C$ ,  $CL$ ,  $\Delta C/CL$  and  $\delta$  are given in the text.

### Introduction

In the last three years, our laboratory has carried out systematically the high-resolution DSC studies of aqueous lipid dispersions prepared individually from some fifty molecular species of saturated diacylphosphatidylcholines with identical or mixed acyl chains. These phospholipids have been grouped into four homologous series, and members of each series share a common molecular weight [1–4]. Interestingly, the main phase transition characteristics of these four series of phospholipids are remarkably similar. Specifically, a common biphasic profile has been detected in all four series of phospholipids, when any one of the thermodynamic parameters ( $T_m$ ,  $\Delta H$ , and  $\Delta S$ ) associated with the main phase transitions is plotted against the ratio of two structural parameters,  $\Delta C/CL$ . Here, the term

$\Delta C$  is the effective chain-length difference, in C-C bonds, between the *sn*-1 and *sn*-2 acyl chains in the diacylphospholipid molecule in the gel-state bilayer and a positive value is assigned for  $\Delta C$ ,  $CL$  is the effective length of the longer one of the two acyl chains, also in C-C bonds, and the ratio of  $\Delta C/CL$  refers to the normalized acyl chain-length difference between the *sn*-1 and *sn*-2 acyl chains for a phospholipid molecule in the gel-state bilayer [1,5].

In the  $T_m$  ( $\Delta H$  or  $\Delta S$ ) vs.  $\Delta C/CL$  plot, the value of  $T_m$  ( $\Delta H$  or  $\Delta S$ ) is observed to decrease with increasing value of  $\Delta C/CL$  up to  $\Delta C/CL \approx 0.42$ ; beyond which the change in  $T_m$  ( $\Delta H$  or  $\Delta S$ ) reverses its direction, thereby resulting in a biphasic V-shaped profile [3,4]. This feature has been postulated to arise from the bulky methyl termini of the lipid acyl chains by perturbing the close van der Waals interactions between acyl chains in the bilayer at  $T < T_m$ . Our recent DSC studies thus have not only characterized the melting behavior for each of the mixed-chain lipids in the four series of phosphatidylcholines in excess water, but also have provided insights and posed questions regarding the perturbing effects of chain terminal methyl groups in the gel-state bilayer.

The linear relationship between the  $T_m$  and  $\Delta C/CL$

Correspondence to: C. Huang, Box 440, Department of Biochemistry, Health Sciences Center, University of Virginia, Charlottesville, VA 22908, USA.

Abbreviations: C(*X*):C(*Y*)PC, saturated 1,2-diacyl-*sn*-glycero-3-phosphocholine with *X* carbons in the *sn*-1 acyl chain and *Y* carbons in the *sn*-2 acyl chain; DSC, differential scanning calorimetry;  $M_r$ , molecular weight;  $T_m$ , the phase transition temperature.

for fully hydrated phosphatidylcholines with  $\Delta C/CL$  values in the range of 0.09–0.40 has been used by Huang [6] to derive a general expression for predicting empirically the  $T_m$  values for identical and mixed-chain phosphatidylcholines. Although this general expression is very successful in predicting the  $T_m$  values for 163 molecular species, it is still rather limited since many mixed-chain phosphatidylcholines have  $\Delta C/CL$  values greater than 0.40.

There is much experimental evidence implicating that saturated mixed-chain phosphatidylcholines with  $\Delta C/CL$  values in the range of 0.42–0.63 self-assemble, in excess water, into the mixed interdigitated bilayer at  $T < T_m$  (Ref. 1 and the references cited therein). This mixed interdigitated bilayer is characterized by the long acyl chain extending fully across the bilayer span, whereas the two shorter chains, each from a lipid in the opposing leaflet, meet end-to-end in the bilayer midplane. Calorimetric results obtained with the four series of asymmetric phosphatidylcholines indicate that the thermodynamic parameters associated with the mixed interdigitated gel  $\rightarrow$  liquid-crystalline phase transitions deviate significantly in the  $T_m$  ( $\Delta H$  or  $\Delta S$ ) vs.  $\Delta C/CL$  plot from the linear function observed for phospholipids with  $\Delta C/CL$  values less than 0.42 [1–4], suggesting that the chain melting behavior of mixed interdigitated bilayers may be governed by structural parameters that contribute differently from those for less asymmetrical lipids. In this communication, we have synthesized some additional phosphatidylcholines with  $\Delta C/CL$  values in the range of 0.43–0.63. The  $T_m$  values of aqueous dispersions prepared from these lipids are analyzed phenomenologically based on the packing model of the mixed interdigitated bilayer. Simple and linear functions of  $T_m$ , in the plot of  $T_m$  vs.  $(\Delta C)^{-1}$ , can be obtained, provided that these mixed-chain phosphatidylcholines are grouped properly. Based on these linear functions, the  $T_m$  values for highly asymmetric mixed-chain phosphatidylcholines with  $\Delta C/CL$  values in the range of 0.43 to 0.63 can be estimated empirically. Consequently, predictions of  $T_m$  values for fully hydrated diacylphosphatidylcholines presented here extend previous work of Huang [6]. It should be mentioned that various linear relationships between the  $T_m$  and the different functions of the inverse of the acyl chain length have been reported previously for saturated diacylphosphatidylcholines [7–10]; in addition, these relationships have been applied successfully to estimate accurately the  $T_m$  values for a large number of phospholipids which undergo the gel  $\rightarrow$  liquid-crystalline phase transitions [10]. The work present here, however, represents the first attempt of predicting  $T_m$  values for highly asymmetric mixed-chain phosphatidylcholines which, in excess water, undergo the mixed interdigitated gel  $\rightarrow$  liquid-crystalline phase transition.

## Experimental procedures

**Materials and routine procedures.** Fatty acids and lysophosphatidylcholines with various acyl chain lengths were purchased from Sigma (St. Louis, MO) and Avanti Polar Lipids, (Birmingham, AL), respectively. Lysophospholipids were stored desiccated at  $-20^\circ\text{C}$ . Silica gel 60 (mesh number: 230–400) was provided by EM Science (Gibbstown, NJ). All common reagents and organic solvents were of reagent and spectroscopic grades, respectively.

Various mixed-chain phosphatidylcholines were prepared at room temperature by acylation of  $\text{CdCl}_2$  adducts of appropriate lysophosphatidylcholines, in dry chloroform, with the anhydrides of desired fatty acids, using 4-pyrrolidinopyridine as the catalyst, and were purified to about 99% purity by repeated column chromatography on Silica gel 60, eluting with chloroform/methanol mixtures. The detailed procedures used for the semisynthesis and purification were the same as those previously employed in this laboratory [2]. Also, the concentrations of all phospholipids were routinely measured as reported previously [2].

**Sample preparation.** Purified lipid was lyophilized from benzene before weighting. The lyophilized lipid from benzene was dispersed in a NaCl (50 mM) aqueous solution containing 5 mM phosphate buffer and 1 mM EDTA at pH 7.4 to give a final lipid concentration in the range of 3.0–6.0 mM. Prior to the DSC experiments, the sample was stored at  $0^\circ\text{C}$  for a minimum of 48 h. All samples were scanned at least three times in the heating direction in the calorimeter. The second and third runs were scanned, if possible, over the temperature range of  $T_m \pm 15^\circ\text{C}$  to ensure identical thermal history of all lipid samples.

**DSC measurements.** Differential scanning calorimetric (DSC) experiments were performed using a high-resolution model MC-2 microcalorimeter equipped with the DA-2 digital interface and data acquisition utility for automatic collection (Microcal, Northampton, MA). In all measurements, a constant heating scan rate of  $15^\circ\text{C}/\text{h}$  was used. Transition temperature ( $T_m$ ) and transition enthalpy ( $\Delta H$ ) were determined from the DSC curve taken from the third heating scan using the software provided by Microcal. In fact, all the thermograms given in various figures in this paper represent the third DSC heating scans for each sample.

## Results and Discussion

### *The structural parameters*

A packing model for the structure of mixed interdigitated gel-state bilayer has been presented consistently by several laboratories [11–13]. This model, schematically shown in Fig. 1, takes into consideration the

following experimental observations obtained with fully hydrated C(18):C(10)PC using the X-ray diffraction technique: (1) The observed bilayer hydrophobic thickness is consistent with the chain length of an all-*trans* C(18) acyl chain; (2) the average headgroup area of C(18):C(10)PC in the gel-state bilayer is about three times the cross-sectional area of an all-*trans* acyl chain; (3) the acyl chains are not tilted in the gel state, since a sharp and symmetric X-ray reflection centered at 4.2 Å is observed in the wide-angle region for fully hydrated C(18):C(10)PC at  $T < T_m$ . The proposed mixed interdigitated bilayer is thus characterized by having the lipid headgroup encompass three hydrocarbon chains, in contrast to the two chains per lipid headgroup for fully hydrated identical-chain phosphatidylcholines in the partially interdigitated gel state (Fig. 1).

Based on the well-known conformation of identical-chain phospholipids in single crystals and in various aggregated states [14], an inherent conformational disparity between the *sn*-1 and the *sn*-2 acyl chains is

assumed for mixed-chain phosphatidylcholines in the mixed interdigitated bilayer. Specifically, the initial segment of the *sn*-2 acyl chain extends parallel to the bilayer surface and then bends over at the bond between C-2 and C-3; thereafter the two acyl chains run parallel along the direction of the bilayer normal. Because of the bend in the *sn*-2 acyl chain, the two terminal methyl ends of an identical-chain phosphatidylcholine molecule in the gel-state bilayer are expected to be mismatched. Indeed, it has been detected by neutron diffraction that the two methyl ends are separated from each other along the long molecular axis by a distance of about 1.5 C-C bonds [15]. In calculating the values of  $\Delta C$  and  $CL$  for mixed-chain phosphatidylcholines, a similar inherent shortening of 1.5 C-C bond lengths has been applied to the apparent chain-length of the *sn*-2 acyl chain [1,6]. This approximation is quite reasonable for mixed-chain phosphatidylcholines with  $\Delta C/CL$  values less than 0.42, since these lipids self-assemble into the gel-state bi-

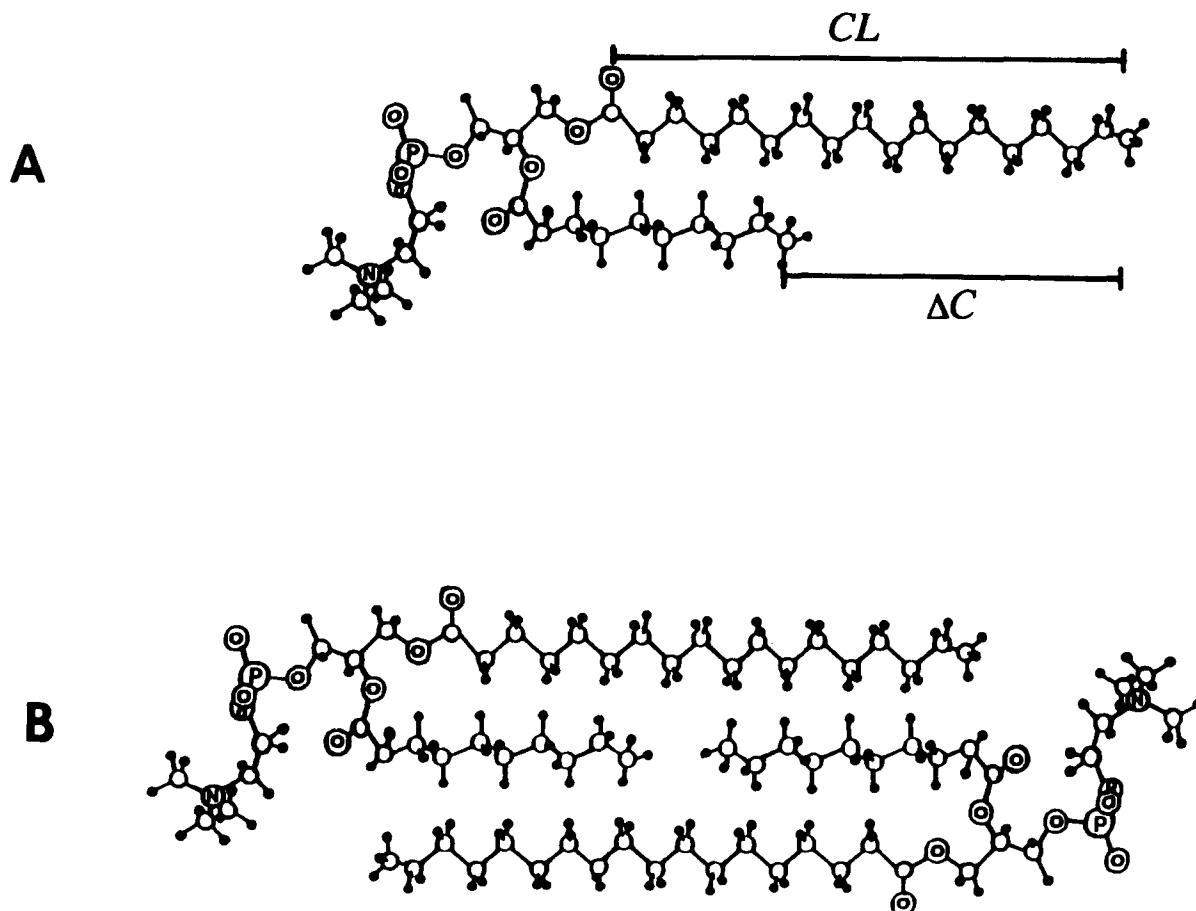


Fig. 1. A schematic representation of the C(18):C(10)PC in the mixed interdigitated gel-state bilayer. (A) The two structural parameters,  $CL$  and  $\Delta C$ , describing the lipid asymmetry are given. It should be noted that the *sn*-2 acyl chains is shorted by  $\sim 1.35$  C-C bond lengths due to an abrupt bend at the C-2 atom near the glycerol backbone region. (B) The molecular packing model of the mixed interdigitated bilayer for C(18):C(10)PC bilayers. It is assumed that the all-*trans* *sn*-1 acyl chain matches perfectly with the effective thickness of two opposing *sn*-2 acyl chains plus the van der Waals distance between the two methyl termini at the bilayer midplane.

layer in a manner which is characteristically similar to the gel-state bilayer comprised of identical-chain phosphatidylcholines. For highly asymmetric phosphatidylcholines with  $\Delta C/CL$  values in the range of 0.43–0.63, the lateral chain-chain interactions in packed lipids in the gel-state bilayer are stronger [16]. In addition, these highly asymmetric phosphatidylcholines are packed in the mixed interdigitated mode at  $T < T_m$  [11–13,17]. Consequently, the assumption that the effective chain length of the *sn*-2 acyl chain is inherently 1.5 C-C bond lengths shorter may not be strictly correct.

A quantitative estimation of the *sn*-2 acyl chain shortening can be obtained indirectly by assuming hydrophobic matching of the lipid acyl chains based on the packing model illustrated in Fig. 1. For a series of mixed-chain phosphatidylcholines in which the *sn*-1 acyl chains are fixed in chain lengths with a total of 18 carbon atoms while the *sn*-2 acyl chains are varied stepwise from 9 to 12 carbon atoms, the normalized transition entropies are known to be very similar [18]; however, the C(18):C(10)PC bilayer has the highest normalized transition entropy [18]. The thermodynamic data thus suggest that within this series of mixed-chain lipid bilayers, the sum of two shorter acyl chain lengths of C(18):C(10)PC plus the close van der Waals contact distance between two opposing chain terminal methyl groups matches most perfectly with the 17 C-C bond lengths of the *sn*-1 C(18)-acyl chain. If we assume that the lateral chain-chain matching is indeed perfect in

C(18):C(10)PC at  $T < T_m$  and if we further assume that the distance between the two opposing terminal methyl groups in the bilayer center is 1.7 C-C bond lengths along the bilayer normal [19], one can readily calculate that the *sn*-2 acyl chain in the mixed interdigitated bilayer is inherently shortened by 1.35 C-C bond lengths in comparison with the *sn*-1 acyl chain. It should be emphasized that this estimated value is calculated based on the molecular packing model of mixed-chain phosphatidylcholines shown in Fig. 1B. In this model, the long axes of lipids' acyl chains in the mixed interdigitated bilayer are normal to the bilayer surface. Based on the estimated shortening of 1.35 C-C bond lengths for the *sn*-2 acyl chain, the  $\Delta C$  and  $\Delta C/CL$  values are subsequently calculated for all other mixed chain phosphatidylcholines which tend to self-assemble into the mixed interdigitated mode at  $T < T_m$ . These new sets of  $\Delta C/CL$  and  $CL$  values are used throughout this communication.

Another structural parameter,  $\delta$ , is the difference between the value of the apparent chain length of the longer acyl chain ( $CL$ ) and the sum of two shorter acyl chains plus the van der Waals contact distance between the two opposing methyl ends [ $2(CL - \Delta C) + 1.7$ ]. The value of  $\delta$  is zero for the mixed interdigitated bilayer of C(18):C(10)PC, since it has been assumed that the longer fully extended acyl chain and the sum of two shorter acyl chains plus the van der Waals contact distance between the two opposing methyl ends are perfectly matched. For various mixed-chain phos-

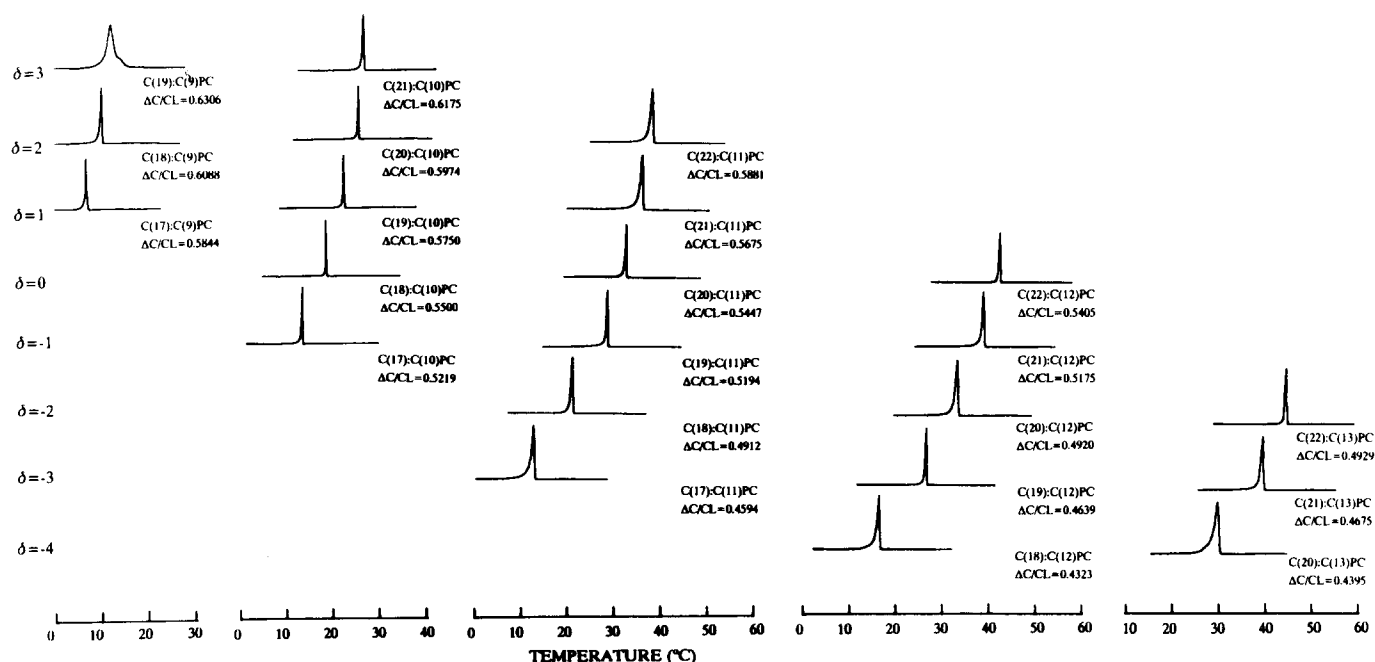


Fig. 2. The third DSC heating curves obtained with aqueous dispersions prepared from five series of highly asymmetrical mixed-chain phosphatidylcholines. The *sn*-1 acyl chain lengths of all these lipids are longer than those of the *sn*-2 acyl chains. Within each series, the *sn*-1 acyl chain increases successively by one methylene unit, while the *sn*-2 acyl chain has a fixed chain length. Scan rate: 15 °C/h. Lipid concentrations: 3–6 mM.

TABLE I

The thermodynamic data associated with the phase transitions of aqueous lipid dispersions prepared from various mixed-chain phosphatidylcholines

$\delta$	Lipid	$\Delta C/CL$	$T_m^{obs}, (^\circ C)$	$\Delta T_{1/2}, (^\circ C)$	$\Delta H, (kcal/mol)$	$\Delta S, (cal/mol \text{ per } K)$
3.0	C(19):C(9)PC	0.6306	13.2	1.75	$8.3 \pm 0.2$	$29.0 \pm 0.7$
	C(21):C(10)PC	0.6175	27.0	0.48	$11.5 \pm 0.4$	$38.3 \pm 1.3$
	C(23):C(11)PC	0.6068	—	—	—	—
	C(25):C(12)PC	0.5979	—	—	—	—
2.0	C(18):C(9)PC	0.6088	11.0	0.46	$8.2 \pm 0.5$	$28.9 \pm 1.7$
	C(20):C(10)PC	0.5974	26.1	0.23	$10.7 \pm 0.5$	$35.7 \pm 1.7$
	C(22):C(11)PC	0.5881	37.5	0.78	$12.2 \pm 0.4$	$39.3 \pm 1.3$
	C(24):C(12)PC	0.5804	—	—	—	—
1.0	C(26):C(13)PC	0.5740	—	—	—	—
	C(17):C(9)PC	0.5844	7.4	0.29	$4.4 \pm 0.5$	$15.7 \pm 1.7$
	C(19):C(10)PC	0.5750	22.7	0.60	$8.3 \pm 0.5$	$28.1 \pm 1.6$
	C(21):C(11)PC	0.5675	35.4	0.80	$12.2 \pm 0.4$	$39.5 \pm 1.3$
0.0	C(23):C(12)PC	0.5614	—	—	—	—
	C(25):C(13)PC	0.5563	—	—	—	—
	C(16):C(9)PC	0.5567	—	—	—	—
	C(18):C(10)PC	0.5500	18.9	0.28	$8.9 \pm 0.3$	$30.5 \pm 1.0$
-1.0	C(20):C(11)PC	0.5447	32.4	0.28	$11.1 \pm 0.6$	$36.3 \pm 2.0$
	C(22):C(12)PC	0.5405	43.1	0.35	$13.2 \pm 0.8$	$41.7 \pm 2.6$
	C(24):C(13)PC	0.5370	—	—	—	—
	C(26):C(14)PC	0.5340	—	—	—	—
-2.0	C(15):C(9)PC	0.5250	—	—	—	—
	C(17):C(10)PC	0.5219	13.6	0.28	$8.4 \pm 0.5$	$29.3 \pm 1.7$
	C(19):C(11)PC	0.5194	28.7	0.35	$11.0 \pm 0.6$	$36.4 \pm 2.0$
	C(21):C(12)PC	0.5175	39.6	0.60	$11.8 \pm 0.3$	$37.7 \pm 1.0$
-3.0	C(23):C(13)PC	0.5159	—	—	—	—
	C(25):C(14)PC	0.5146	—	—	—	—
	C(14):C(9)PC	0.4885	—	—	—	—
	C(16):C(10)PC	0.4900	—	—	—	—
-4.0	C(18):C(11)PC	0.4912	21.35	0.48	$9.1 \pm 0.5$	$30.9 \pm 1.7$
	C(20):C(12)PC	0.4921	34.2	0.80	$11.5 \pm 0.6$	$37.4 \pm 2.0$
	C(22):C(13)PC	0.4929	44.6	0.53	$14.1 \pm 0.7$	$44.4 \pm 2.2$
	C(24):C(14)PC	0.4935	—	—	—	—
-5.0	C(26):C(15)PC	0.4940	—	—	—	—
	C(13):C(9)PC	0.4458	—	—	—	—
	C(15):C(10)PC	0.4536	—	—	—	—
	C(17):C(11)PC	0.4594	12.8	0.80	$6.9 \pm 0.5$	$24.1 \pm 1.8$
-6.0	C(19):C(12)PC	0.4639	27.7	0.33	$9.6 \pm 0.4$	$31.9 \pm 1.3$
	C(21):C(13)PC	0.4675	39.4	0.72	$12.0 \pm 0.5$	$38.4 \pm 1.6$
	C(23):C(14)PC	0.4705	—	—	—	—
	C(25):C(15)PC	0.4729	—	—	—	—
-7.0	C(18):C(12)PC	0.4320	17.3	0.68	$8.4 \pm 0.8$	$28.9 \pm 2.8$
	C(20):C(13)PC	0.4395	30.2	1.11	$11.6 \pm 0.5$	$38.2 \pm 1.7$
	C(22):C(14)PC	0.4452	41.3	1.15	$13.7 \pm 0.7$	$43.6 \pm 2.2$
	C(24):C(15)PC	0.4500	—	—	—	—
-8.0	C(26):C(16)PC	0.4540	—	—	—	—
	C(8):C(21)PC	0.6247	24.3	0.71	$10.7 \pm 0.4$	$36.5 \pm 0.9$
	C(9):C(23)PC	0.6126	33.7	0.38	$11.4 \pm 0.3$	$37.2 \pm 0.9$
	C(10):C(25)PC	0.6026	43.1	0.53	$13.1 \pm 0.6$	$41.4 \pm 1.9$
-9.0	C(8):C(20)PC	0.6034	21.3	0.25	$12.2 \pm 0.9$	$41.4 \pm 3.1$
	C(9):C(22)PC	0.5929	32.0	0.90	$11.5 \pm 0.4$	$37.7 \pm 1.3$
	C(10):C(24)PC	0.5843	42.2	0.72	$13.3 \pm 0.2$	$42.2 \pm 0.6$
	C(11):C(26)PC	0.5772	—	—	—	—
-10.0	C(8):C(19)PC	0.5796	17.1	0.33	$10.2 \pm 0.2$	$35.1 \pm 0.7$
	C(9):C(21)PC	0.5710	29.3	0.47	$11.2 \pm 0.3$	$36.4 \pm 1.0$
	C(10):C(23)PC	0.5642	40.0	0.70	$13.2 \pm 0.5$	$42.2 \pm 1.6$
	C(11):C(25)PC	0.5585	49.5	0.29	$13.7 \pm 0.5$	$42.5 \pm 1.5$
-11.0	C(8):C(18)PC	0.5527	10.2	0.50	$7.1 \pm 0.6$	$25.0 \pm 2.2$
	C(9):C(20)PC	0.5467	24.9	0.28	$10.9 \pm 0.7$	$36.9 \pm 2.0$
	C(10):C(22)PC	0.5420	37.4	0.28	$11.9 \pm 0.7$	$38.3 \pm 2.3$
	C(11):C(24)PC	0.5381	47.7	0.50	$13.4 \pm 0.7$	$41.8 \pm 2.1$
-12.0	C(12):C(26)PC	0.5349	55.2	0.85	$14.7 \pm 0.3$	$44.8 \pm 0.9$

TABLE 1 (continued)

$\delta$	Lipid	$\Delta C/CL$	$T_m^{obs}, (^\circ C)$	$\Delta T_{1/2}, (^\circ C)$	$\Delta H, (kcal/mol)$	$\Delta S, (cal/mol \text{ per } K)$
-1.05	C(8):C(17)PC	0.5222	—	—	—	—
	C(9):C(19)PC	0.5195	19.6	0.88	$11.3 \pm 0.9$	$38.6 \pm 3.1$
	C(10):C(21)PC	0.5174	32.7	0.27	$11.3 \pm 0.3$	$36.9 \pm 1.0$
	C(11):C(23)PC	0.5157	43.5	0.55	$12.4 \pm 0.3$	$39.2 \pm 0.9$
	C(12):C(25)PC	0.5143	—	—	—	—
-2.05	C(9):C(18)PC	0.4888	10.9	0.66	$8.3 \pm 0.6$	$29.2 \pm 2.0$
	C(10):C(20)PC	0.4901	26.8	0.28	$9.2 \pm 0.7$	$30.7 \pm 2.3$
	C(11):C(22)PC	0.4911	38.6	0.45	$12.6 \pm 0.2$	$40.4 \pm 0.7$
	C(12):C(24)PC	0.4919	48.7	0.43	$13.8 \pm 0.5$	$42.9 \pm 1.5$
	C(13):C(26)PC	0.4926	—	—	—	—
-3.05	C(9):C(17)PC	0.4539	—	—	—	—
	C(10):C(19)PC	0.4595	19.9	0.53	$7.1 \pm 0.5$	$24.2 \pm 1.7$
	C(11):C(21)PC	0.4638	32.6	0.58	$9.4 \pm 0.4$	$30.7 \pm 1.4$
	C(12):C(23)PC	0.4673	44.0	0.82	$13.4 \pm 0.4$	$42.3 \pm 1.2$
	C(13):C(25)PC	0.4702	53.3	0.45	$14.7 \pm 0.4$	$45.0 \pm 1.3$
-4.05	C(10):C(18)PC	0.4249	—	—	—	—
	C(11):C(20)PC	0.4334	25.7	0.50	$8.4 \pm 0.2$	$28.1 \pm 0.7$
	C(12):C(22)PC	0.4402	37.6	0.68	$13.2 \pm 0.3$	$42.5 \pm 0.9$
	C(13):C(24)PC	0.4457	—	—	—	—
	C(14):C(26)PC	0.4503	55.5	0.91	$15.1 \pm 0.5$	$45.9 \pm 1.6$

phatidylcholines which can form mixed interdigitated bilayers,  $\delta$  value can be either positive or negative, depending on the values of CL and  $[2(CL - \Delta C) + 1.7]$ .

*Thermotropic phase behavior of homologous series of mixed-chain phosphatidylcholines with longer sn-1 acyl chains and with  $\Delta C/CL$  values in the range of 0.43–0.63*

To study systematically the melting behavior of various mixed-chain phosphatidylcholines packed in the mixed interdigitated gel-state, we have first performed the high-resolution DSC studies on five series of phosphatidylcholines with  $\Delta C/CL$  values in the range of 0.43–0.63. The *sn*-1 acyl chain lengths of all these lipids are longer than those of the *sn*-2 acyl chains. In fact, the *sn*-2 acyl chain length increases systematically from 9 to 13 in these 5 series of lipids. Within each series, however, the *sn*-1 acyl chain increases successively by one methylene unit.

Fig. 2 shows some typical DSC curves obtained with lipid samples after the third DSC heating scans. The corresponding values of  $\Delta C/CL$  and  $\delta$  are also indicated. With the exception of C(19):C(9)PC, all lipid samples exhibit a single, sharp, endothermic peak upon heating. In fact, these endothermic transition curves are, within experimental errors, independent of the thermal history of the lipid samples. Moreover, these samples do not exhibit the subtransition or the pretransition upon initial heating. Hence, the observed single endothermic transition for each of the mixed-chain phosphatidylcholines shown in Fig. 2 can be ascribed to the mixed interdigitated gel to the liquid-crystalline phase transition [3,19].

The phase transition characteristics of these five homologous series of mixed-chain phosphatidylcholines are very similar. The value of  $T_m$  in each series increases steadily with increasing *sn*-1 acyl chain length; however, the increase becomes progressively smaller as the  $\delta$  value increases successively (Fig. 2). The transition peak width at half-height ( $\Delta T_{1/2}$ ) also varies within each series, but the observed sharpest transition curve is invariably the one with a  $\delta$  value of zero. The experimental values of  $T_m$ ,  $\Delta H$ ,  $\Delta S$  and  $\Delta T_{1/2}$  associated with the phase transitions of the aqueous dispersions prepared from 23 mixed-chain phosphatidylcholines with longer acyl chains at the *sn*-1 position of the glycerol backbone are summarized in Table I.

In Fig. 3, the  $T_m$  values of various lipid dispersions listed in Table I are plotted against  $1/\Delta C$ . Clearly, the values of  $T_m$  from each homologous series of lipids give rise to a smooth curvilinear curve. However, a closer examination of the data given in Fig. 3 reveals an interesting feature. When the various  $T_m$  values corresponding to mixed-chain phosphatidylcholines with a common  $\delta$  value are connected, a grid of linear curves is obtained. Considering, for example, C(18):C(11)PC, C(20):C(12)PC, and C(22):C(13)PC, these lipids have a common  $\delta$  value of  $-2$ , and the least-squares line best fitting their  $T_m$  values in the  $T_m$  vs.  $1/\Delta C$  plot has the form:  $T_m = -1002.22(1/\Delta C) + 141.42$  with a correlation coefficient of 1.0. The  $T_m$  value of C(16):C(10)PC ( $1/\Delta C = 0.1361$ ,  $\delta = -2$ ) can be calculated from the least-squares expression to be  $5.0^\circ C$ . This calculated value is in excellent agreement with the experimental value of  $4.9^\circ C$  [19], indicating

TABLE II

Predicted and calculated  $T_m$  values for various mixed-chain phosphatidylcholines based on experimental  $T_m$  values determined calorimetrically

$\delta$	Lipid	$\Delta C/CL$	$(\Delta C)^{-1}$	$T_m^{\text{obs}} (^{\circ}C)$	$T_m^{\text{cal}} (^{\circ}C)$	$T_m^{\text{prd}} (^{\circ}C)$	$\Delta T_m (C^{\circ})^a$
3.0	C(19):C(9)PC	0.6306	0.0881	13.2	13.2	12.6	-0.6
	C(21):C(10)PC	0.6175	0.0810	27.0	27.0	26.3	-0.7
	C(23):C(11)PC	0.6068	0.0749	-	38.9	38.1	-
	C(25):C(12)PC	0.5979	0.0697	-	49.0	48.1	-
2.0	C(18):C(9)PC	0.6088	0.0966	11.0	11.2	11.8	0.8
	C(20):C(10)PC	0.5974	0.0881	26.1	25.7	26.4	0.3
	C(22):C(11)PC	0.5881	0.0810	37.5	37.7	38.5	1.0
	C(24):C(12)PC	0.5804	0.0749	-	48.1	49.0	-
1.0	C(26):C(13)PC	0.5740	0.0697	-	57.0	57.9	-
	C(17):C(9)PC	0.5844	0.1070	7.4	7.4	8.1	0.7
	C(19):C(10)PC	0.5750	0.0966	22.7	22.8	23.6	0.9
	C(21):C(11)PC	0.5675	0.0881	35.4	35.4	36.2	0.8
0.0	C(23):C(12)PC	0.5614	0.0810	-	45.9	46.8	-
	C(25):C(13)PC	0.5563	0.0749	-	54.9	55.9	-
	C(16):C(9)PC	0.5567	0.1198	-	2.6	1.9	-
	C(18):C(10)PC	0.5500	0.1070	18.9	19.0	18.2	-0.7
-1.0	C(20):C(11)PC	0.5447	0.0966	32.4	32.3	31.4	-1.0
	C(22):C(12)PC	0.5405	0.0881	43.1	43.2	42.2	-0.9
	C(24):C(13)PC	0.5370	0.0810	-	52.3	51.2	-
	C(26):C(14)PC	0.5340	0.0749	-	60.1	59.0	-
-2.0	C(15):C(9)PC	0.5250	0.1361	-	-4.5	-4.4	-
	C(17):C(10)PC	0.5219	0.1198	13.6	13.8	13.9	0.3
	C(19):C(11)PC	0.5194	0.1070	28.7	28.2	28.2	-0.5
	C(21):C(12)PC	0.5175	0.0966	39.6	39.9	39.8	0.2
-3.0	C(23):C(13)PC	0.5159	0.0881	-	49.4	49.3	-
	C(25):C(14)PC	0.5146	0.0810	-	57.4	57.3	-
	C(14):C(9)PC	0.4885	0.1575	-	-16.4	-16.5	-
	C(16):C(10)PC	0.4900	0.1361	-	5.0	5.3	-
-4.0	C(18):C(11)PC	0.4912	0.1198	21.35	21.4	21.9	0.5
	C(20):C(12)PC	0.4921	0.1070	34.2	34.2	34.9	0.7
	C(22):C(13)PC	0.4929	0.0966	44.6	44.6	45.5	0.9
	C(24):C(14)PC	0.4935	0.0881	-	53.1	54.2	-
-5.0	C(26):C(15)PC	0.4940	0.0810	-	60.2	61.4	-
	C(13):C(9)PC	0.4458	0.1869	-	-33.6	-32.9	-
	C(15):C(10)PC	0.4536	0.1575	-	-6.8	-5.9	-
	C(17):C(11)PC	0.4594	0.1361	12.8	12.8	13.8	1.0
-6.0	C(19):C(12)PC	0.4639	0.1198	27.7	27.7	28.7	1.0
	C(21):C(13)PC	0.4675	0.1070	39.4	39.4	40.5	1.1
	C(23):C(14)PC	0.4705	0.0966	-	48.9	50.0	-
	C(25):C(15)PC	0.4729	0.0881	-	56.7	57.8	-
-7.0	C(18):C(12)PC	0.4320	0.1361	17.3	17.1	17.0	-0.3
	C(20):C(13)PC	0.4395	0.1198	30.2	30.6	30.4	0.2
	C(22):C(14)PC	0.4452	0.1070	41.3	41.1	40.8	-0.5
	C(24):C(15)PC	0.4500	0.0966	-	49.7	49.4	-
-8.0	C(26):C(16)PC	0.4540	0.0881	-	56.7	56.3	-
	C(8):C(21)PC	0.6247	0.0858	24.3	24.1	24.5	0.2
	C(9):C(23)PC	0.6126	0.0791	33.7	34.2	34.7	1.0
	C(10):C(25)PC	0.6026	0.0733	43.1	42.9	43.4	0.3
-9.0	C(8):C(20)PC	0.6034	0.0939	21.3	21.1	21.1	-0.2
	C(9):C(22)PC	0.5929	0.0858	32.0	32.5	32.5	0.5
	C(10):C(24)PC	0.5843	0.0791	42.2	41.9	42.0	-0.2
	C(11):C(26)PC	0.5772	0.0733	-	50.1	50.2	-
-10.0	C(8):C(19)PC	0.5796	0.1036	17.1	16.8	16.4	-0.7
	C(9):C(21)PC	0.5710	0.0939	29.3	29.6	29.2	-0.1
	C(10):C(23)PC	0.5642	0.0858	40.0	40.3	39.8	-0.2
	C(11):C(25)PC	0.5585	0.0791	49.5	49.2	48.6	-0.9
-11.0	C(8):C(18)PC	0.5527	0.1156	10.2	10.2	10.3	0.1
	C(9):C(20)PC	0.5467	0.1036	24.9	25.1	24.9	0.0
	C(10):C(22)PC	0.5420	0.0939	37.4	37.2	36.6	-0.8
	C(11):C(24)PC	0.5381	0.0858	47.7	47.3	46.5	-1.2
-12.0	C(12):C(26)PC	0.5349	0.0791	55.2	55.6	54.6	-0.6

TABLE II (continued)

$\delta$	Lipid	$\Delta C/CL$	$(\Delta C)^{-1}$	$T_m^{obs}$ ( $^{\circ}C$ )	$T_m^{cal}$ ( $^{\circ}C$ )	$T_m^{prd}$ ( $^{\circ}C$ )	$\Delta T_m$ ( $^{\circ}C$ ) <sup>a</sup>
-1.05	C(8):C(17)PC	0.5222	0.1307	—	2.9	2.1	—
	C(9):C(19)PC	0.5195	0.1156	19.6	19.6	18.9	-0.7
	C(10):C(21)PC	0.5174	0.1036	32.7	32.8	32.3	-0.4
	C(11):C(23)PC	0.5157	0.0939	43.5	43.5	43.1	-0.4
	C(12):C(25)PC	0.5143	0.0858	—	52.4	52.1	—
-2.05	C(9):C(18)PC	0.4888	0.1307	10.9	11.0	11.2	0.3
	C(10):C(20)PC	0.4901	0.1156	26.8	26.5	26.6	-0.2
	C(11):C(22)PC	0.4911	0.1036	38.6	38.8	38.7	0.1
	C(12):C(24)PC	0.4919	0.0939	48.7	48.7	48.5	-0.2
	C(13):C(26)PC	0.4926	0.0858	—	57.0	56.8	—
-3.05	C(9):C(17)PC	0.4539	0.1504	—	1.6	1.1	—
	C(10):C(19)PC	0.4595	0.1307	19.9	19.5	19.1	-0.8
	C(11):C(21)PC	0.4638	0.1156	32.6	33.2	32.9	0.3
	C(12):C(23)PC	0.4673	0.1036	44.0	44.1	43.8	-0.2
	C(13):C(25)PC	0.4702	0.0939	53.3	52.9	52.7	-0.6
-4.05	C(10):C(18)PC	0.4249	0.1504	—	9.6	9.4	—
	C(11):C(20)PC	0.4334	0.1307	25.7	25.6	25.4	-0.3
	C(12):C(22)PC	0.4402	0.1156	37.6	37.8	37.7	0.1
	C(13):C(24)PC	0.4457	0.1036	—	47.5	47.4	—
	C(14):C(26)PC	0.4503	0.0939	55.5	55.4	55.3	-0.2

<sup>a</sup> The difference in  $T_m$  between the predicted ( $T_m^{prd}$ ) and the experimentally observed ( $T_m^{obs}$ ) values.

that the least-squares lines in Fig. 3 may be used feasibly as a means to calculate the  $T_m$  values for a number of mixed-chain phosphatidylcholines. Consequently, the calculated  $T_m$  values for many mixed-chain phosphatidylcholines are evaluated by the same least-squares procedure, and the results are given in the column labeled  $T_m^{cal}$  in Table II. The slopes and Y-intercepts of these least-squares lines are summarized in Table III.

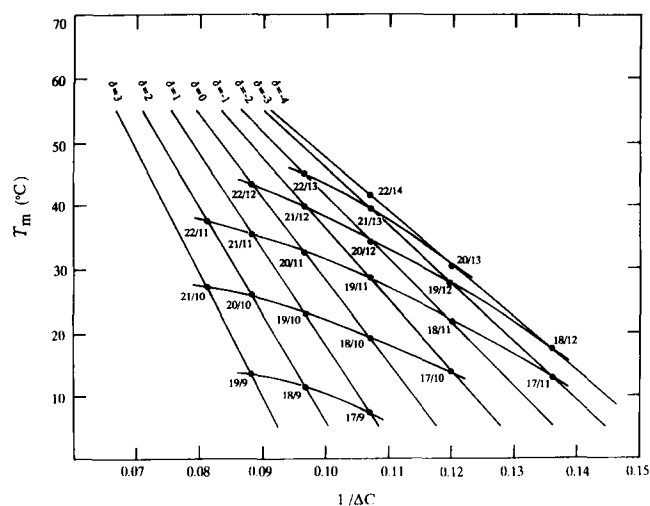


Fig. 3. The phase transition temperature ( $T_m$ ) versus  $(\Delta C)^{-1}$  for various highly asymmetrical mixed-chain phosphatidylcholines with longer *sn*-1 acyl chains. The *X/Y* pair-number under each experimental point denotes the individual mixed-chain phosphatidylcholine with *X* and *Y* carbons in the *sn*-1 and the *sn*-2 acyl chains, respectively.

*Thermodynamic phase behavior of mixed-chain phosphatidylcholines with longer sn-2 acyl chains and with  $\Delta C/CL$  values in the range of 0.43–0.65*

The next set of DSC experiments was aimed at finding out whether a switch in the relative chain lengths in the *sn*-1 and the *sn*-2 positions would have an effect on the phase transition behavior for mixed-chain phosphatidylcholines with  $\Delta C/CL$  values in the range of 0.43–0.63. In these experiments, the mixed-chain phospholipids have longer acyl chains at the *sn*-2

TABLE III

The slopes (*m*) and ratios of the Y-axis intercept / slope (*b/m*) of the various least-squares lines best-fitting the  $T_m$  values at given values of  $\delta$  as shown in Figs. 3 and 5

$\delta$	<i>m</i>	<i>b/m</i>
3.0	-1943.662	-0.095
2.0	-1701.246	-0.103
1.0	-1481.102	-0.112
0.0	-1281.072	-0.122
-1.0	-1122.927	-0.132
-2.0	-1002.222	-0.141
-3.0	-914.090	-0.150
-4.0	-823.252	-0.157
2.95	-1501.406	-0.102
1.95	-1409.025	-0.109
0.95	-1319.470	-0.116
-0.05	-1243.612	-0.124
-1.05	-1101.004	-0.133
-2.05	-1023.453	-0.142
-3.05	-908.965	-0.152
-4.05	-810.836	-0.162



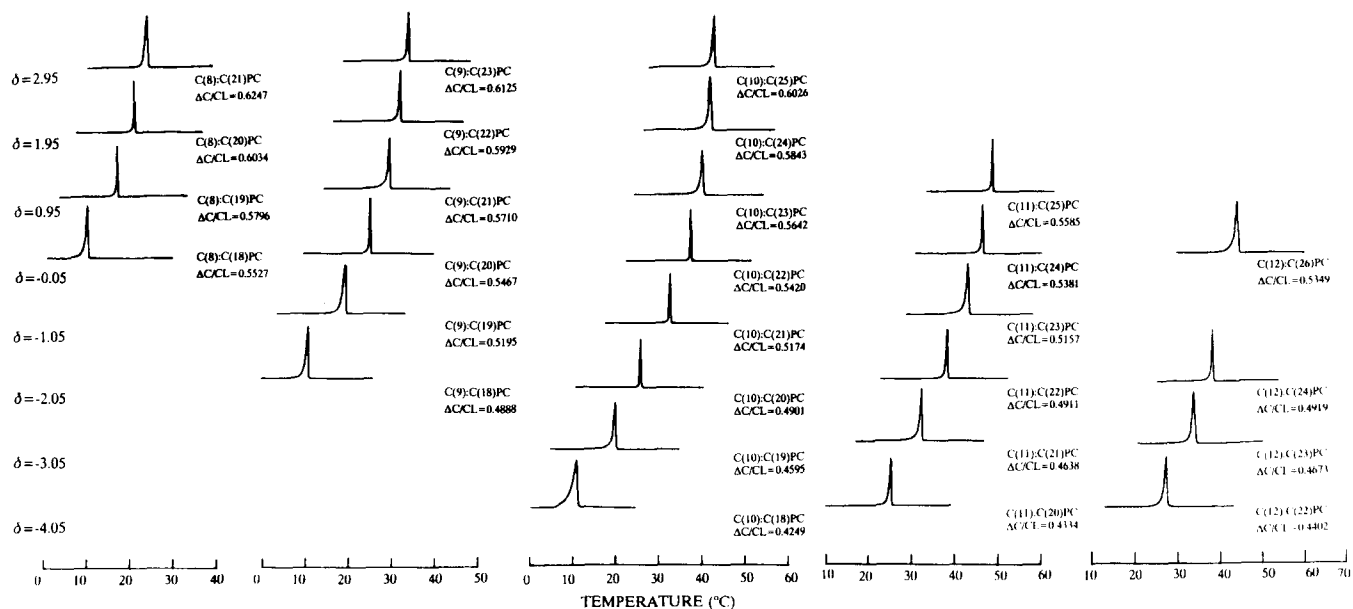


Fig. 4. The third DSC heating curves obtained with aqueous dispersions prepared from five series of highly asymmetrical mixed-chain phosphatidylcholines with longer *sn*-2 acyl chains. See Fig. 2 legend for experimental conditions.

position of the glycerol backbone. In addition, both the acyl chain lengths at the *sn*-1 and the *sn*-2 positions of the glycerol backbone are systematically modified.

Some typical DSC heating thermograms obtained with aqueous dispersions prepared from five homologous series of mixed-chain phosphatidylcholines with longer *sn*-2 acyl chains and with  $\Delta C/CL$  values in the range of 0.43–0.63 are illustrated in Fig. 4. All samples exhibit a sharp, single, endothermic transition upon heating. It is evident that within each series the upward shift in  $T_m$  decreases progressively as the *sn*-2 acyl chain length increases successively. In addition, the sharpest transition peak is displayed by the lipid species with the smallest absolute value of  $\delta$ . These phase transition characteristics are thus remarkably similar to those exhibited by mixed-chain phosphatidylcholines which have longer *sn*-1 acyl chains as shown in Fig. 2. The thermodynamic parameters associated with the main phase transitions for 29 mixed-chain phosphatidylcholines including all those shown in Fig. 4 are summarized in Table I.

Analysis of the  $T_m$  values for all the mixed-chain phosphatidylcholines with shorter *sn*-1 acyl chains reveals a linear relationship between  $T_m$  and  $1/\Delta C$  at a common value of  $\delta$  (Fig. 5). For instance, C(9):C(18)PC, C(10):C(20)PC, C(11):C(22)PC and C(12):C(24)PC have a common  $\delta$  value of  $-2.05$ . The least-squares line best fitting their  $T_m$  values has the expression:  $T_m = -1023.45(1/\Delta C) + 144.80$ , with a correlation coefficient of 0.9999. This expression can then be used to calculate the  $T_m$  values for C(8):C(16)PC and C(13):C(26)PC, and the results,  $-9.1^\circ\text{C}$  and  $57.0^\circ\text{C}$ , respectively, are listed in Table II under the label  $T_m^{\text{cal}}$ .

The slopes and Y-intercepts of all the least-squares lines best fitting the experimental  $T_m$  values for various lipids at given values of  $\delta$  are listed in Table III.

#### Empirical equations for predicting the $T_m$ values

A key feature of the results shown in Figs. 3 and 5 is that the values of  $T_m$  for various phosphatidylcholines at constant values of  $\delta$  are linear functions of  $1/\Delta C$ . As discussed in the preceding sections, these linear curves can be used individually to calculate the  $T_m$  values for mixed-chain phosphatidylcholines at a constant value of  $\delta$ . If, however, a common relationship can be sought between all these lines and their corre-

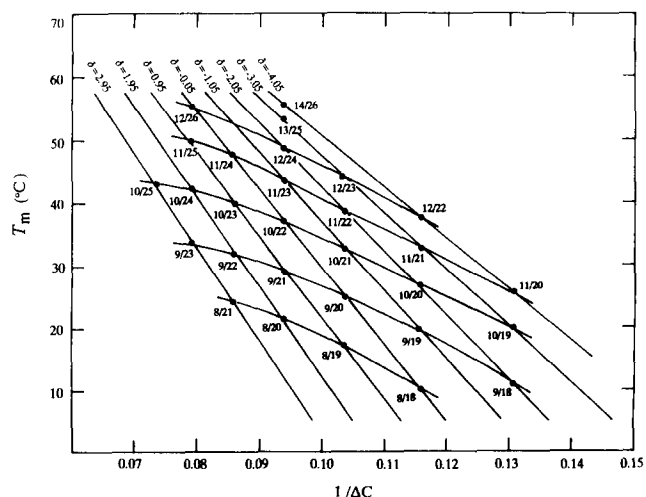


Fig. 5. The phase transition temperature ( $T_m$ ) versus  $(\Delta C)^{-1}$  for various highly asymmetrical mixed-chain phosphatidylcholines with longer *sn*-2 acyl chains. See Fig. 3 legend for other notations.

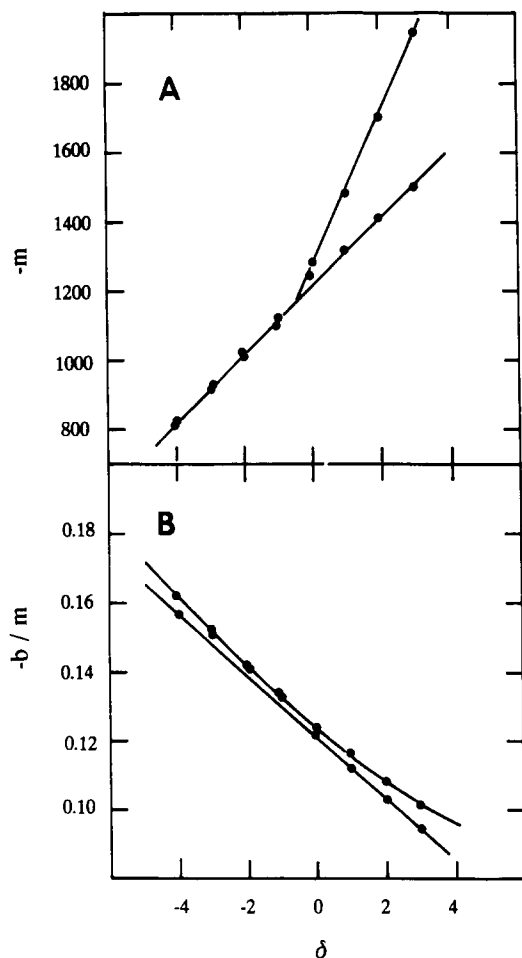


Fig. 6. The plot of the negative slope ( $-m$ ) or the negative ratio of the Y-intercept/slope ( $-b/m$ ) of the various linear curves shown in Figs. 3 and 5 against the structural parameter of  $\delta$ .

sponding  $\delta$  values, then a general equation relating  $T_m$ ,  $\delta$ , and  $1/\Delta C$  perhaps can be derived. If so, the prediction of  $T_m$  value for mixed-chain phosphatidylcholines with  $\Delta C/CL$  values in the range of 0.43–0.63 can be greatly simplified. Here, we first derive the general equations, and, then, compare the calculated  $T_m$  values with the observed ones.

The slopes,  $m$ , and the ratios of the Y-intercept/slope,  $b/m$ , of the various linear curves at constant values of  $\delta$  observed in Figs. 3 and 5 are plotted against  $\delta$  in Figs. 6A and B, respectively. In Fig. 6A, all the data points of  $m$  are seen to fall on two straight lines. The point corresponding to a  $\delta$  value of  $-0.05$ , however, can fit into either line. We place this point into the larger group of data points to form the lower straight line in Fig. 6A. These 12 data points can be best fit by the least-squares to an equation of the form:  $m = -99.9538(\delta) - 1218.2997$  with a correlation coefficient of 0.9985. The other four values of  $m$  obtained with mixed-chain phosphatidylcholines with integral values of  $\delta$  ranging from 0 to 3 fall on a different straight line; the least-squares expression takes the

form:  $m = -220.7914(\delta) - 1270.5834$  with a correlation coefficient of 0.9991. The ratios of the Y-intercept/slope,  $b/m$ , of the various linear curves observed in Figs. 3 and 5 are plotted in Fig. 6B versus  $\delta$ . Again, these data can be fit into two curves. The values of  $b/m$  obtained with five series of mixed-chain phosphatidylcholines which have  $\delta$  values of  $-4$ , 0, 1, 2, and 3, respectively, can be fit into a linear function of  $\delta$  as follows:  $b/m = 8.9 \cdot 10^{-3}(\delta) - 0.1213$  with a correlation coefficient of 0.9999. All the other data points, however, fall on a nonlinear curve (Fig. 6B) and a least-squares expression of  $b/m = -0.1237 + 8.2320 \cdot 10^{-3}(\delta) - 2.987 \cdot 10^{-4}(\delta)^2$  with a correlation coefficient of 0.9997 can be yielded to fit these eleven data points. The least-squares functions of the four curves shown in Figs. 6A and B can be summarized as follows:

For  $\delta = 0, 1, 2$ , and 3:

$$m = -220.7914(\delta) - 1270.5834$$

$$b/m = 8.9 \cdot 10^{-3}(\delta) - 0.1213$$

For  $\delta = -4.05, -3.05, -3.00, -2.05, -2.00, -1.05, -1.00, -0.05, 0.95, 1.95$  and 2.95:

$$m = -99.9538(\delta) - 1218.2993$$

$$b/m = -0.1237 + 8.2320 \cdot 10^{-3}(\delta) - 2.987 \cdot 10^{-4}(\delta)^2$$

For  $\delta = -4$ :

$$m = -99.9538(\delta) - 1218.2993$$

$$b/m = 8.9 \cdot 10^{-3}(\delta) - 0.1213$$

Substituting these least-squares functions into the equation  $T_m = m(\Delta C)^{-1} + b = m[(\Delta C)^{-1} + b/m]$ , the general equations for the phase transition temperature for mixed-chain phosphatidylcholines with different  $\delta$  values are obtained:

For  $\delta = 0, 1, 2$ , and 3:

$$T_m = [-220.7914(\delta) - 1270.5834][(\Delta C)^{-1} + 8.9 \cdot 10^{-3}(\delta) - 0.1213]$$

For  $\delta = -4.05, -3.05, -3.00, -2.05, -2.00, -1.05, -1.00, -0.05, 0.95, 1.95$  and 2.95:

$$T_m = [-99.9538(\delta) - 1218.2993]$$

$$\times [(\Delta C)^{-1} - 0.1237 + 8.2320 \cdot 10^{-3}(\delta) - 2.987 \cdot 10^{-4}(\delta)^2]$$

For  $\delta = -4$ :

$$T_m = [-99.9538(\delta) - 1218.2993][(\Delta C)^{-1} + 8.9 \cdot 10^{-3}(\delta) - 0.1213]$$

Based on these general empirical equations, the predicted  $T_m$  values for all mixed-chain phosphatidylcholines with  $\delta$  values in the range of  $-4.05$  to  $3.00$  can be evaluated; the resulting values are presented as  $T_m^{\text{prd}}$  in Table II. It is evident from these empirical

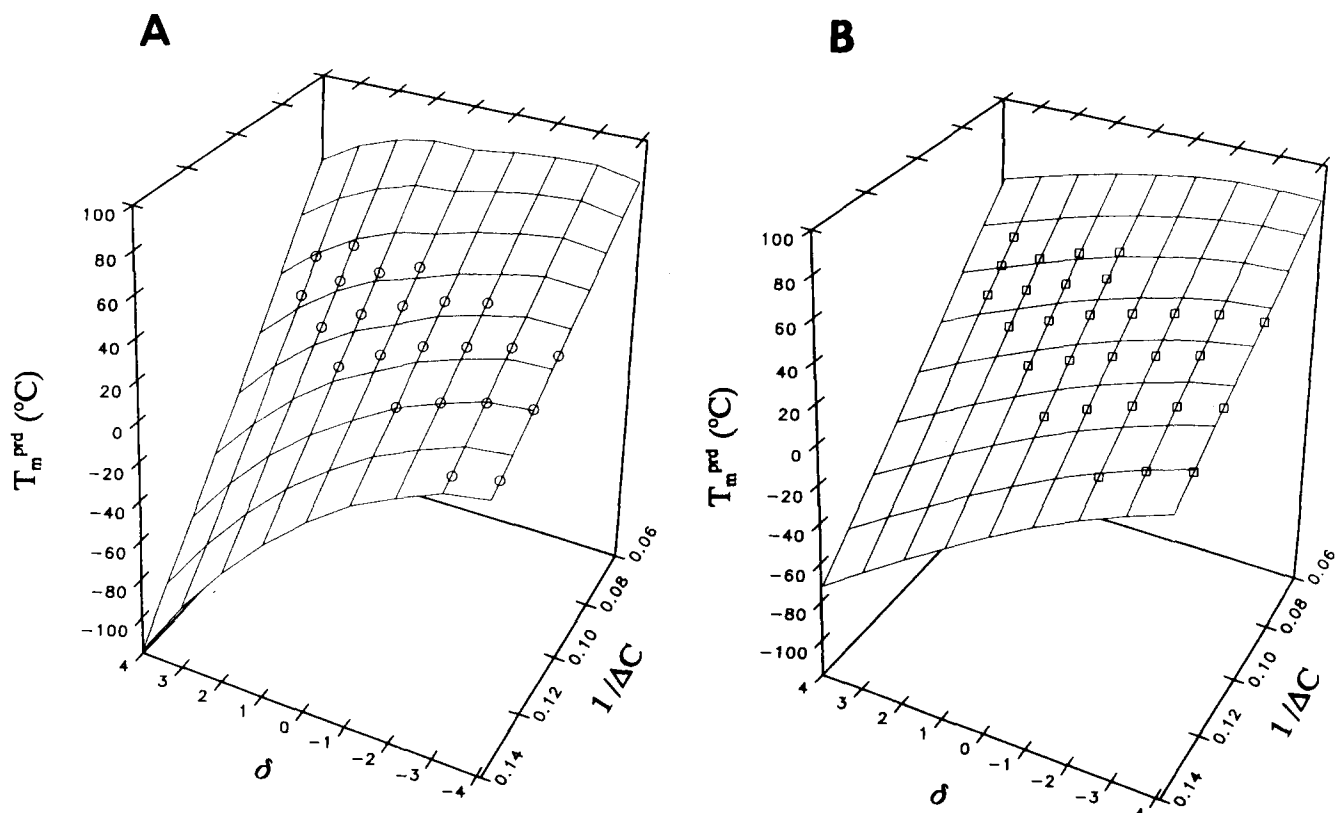


Fig. 7. Three-dimensional pictures showing the  $T_m^{\text{prd}}$ -surfaces as a function of the two structural parameters ( $\delta$  and  $1/\Delta C$ ). (A) The  $T_m^{\text{prd}}$ -surface for highly asymmetrical mixed-chain phosphatidylcholines with longer *sn*-1 acyl chains. (B) The  $T_m^{\text{prd}}$ -surface for highly asymmetrical mixed-chain phosphatidylcholines with longer *sn*-2 acyl chains. Both three-dimensional surfaces are generated based on the prediction equations derived in the text. The circles and squares are experimentally observed  $T_m$  values.

equations that the  $T_m^{\text{prd}}$  value of a given highly asymmetrical mixed-chain phosphatidylcholine depends on the structural parameters of  $\delta$  and  $(\Delta C)^{-1}$ . These expressions are different from the general equation of Huang [6] used previously in predicting the  $T_m$  values for less asymmetrical mixed-chain phosphatidylcholines with  $\Delta C/\text{CL}$  values in the range of 0.09 to 0.40; the latter depends on the structural parameters of  $\Delta C$ ,  $(\text{CL})^{-1}$  and  $\Delta C/\text{CL}$  [6]. For highly asymmetrical mixed-chain phosphatidylcholines with  $\Delta C/\text{CL}$  values in the range of 0.43–0.63, the concomitant dependence of  $T_m^{\text{prd}}$  on both  $\delta$  and  $(\Delta C)^{-1}$  is demonstrated graphically in two three-dimensional figures as illustrated in Fig. 7. The two-dimensional surfaces of  $T_m^{\text{prd}}$  for highly asymmetrical mixed-chain phospholipids with longer *sn*-1 acyl chains and for those with longer *sn*-2 acyl chains are presented in Figs. 7A and 7B, respectively.

The experimental  $T_m$  values for all the mixed-chain phosphatidylcholines under current DSC study are plotted in Fig. 8 versus the predicted values. Clearly, the comparison indicates that the agreement is excellent in all cases. Of the 52 pairs of data compared, the largest deviation between the predicted and observed  $T_m$  values is observed for C(11):C(24)PC (Fig. 8 and Table II); this largest deviation, 1.2 °C, corresponds to a relative error of 2.5% in °C or a relative error of

0.4% in absolute temperature. Thus the predicted  $T_m$  values listed in Table II for mixed-chain phosphatidylcholines with  $\delta$  values in the range of  $-4.05$  to  $3.00$

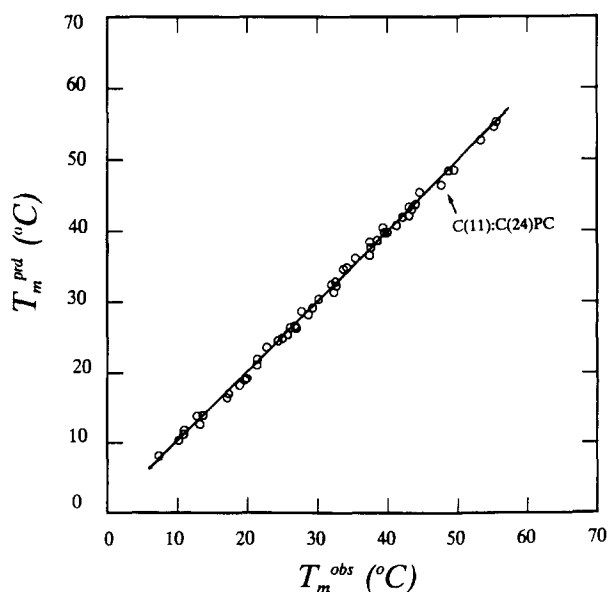


Fig. 8. Comparison of the predicted  $T_m^{\text{prd}}$  values and the experimentally observed  $T_m^{\text{obs}}$  values. Of the 52 pairs of data compared, only C(11):C(24)PC shows the greatest deviation of 1.2 °C as indicated.

are most likely to be the representative of those known accurately by high-resolution DSC experiments. These predicated  $T_m$  values can be readily calculated from the general equations derived earlier.

## Conclusions

Phosphatidylcholines, a major lipid component of biological membranes, consist of a large number of molecular species characterized by different acyl chains. If we consider only the saturated diacylphosphatidylcholines with each of the two chains limited to a range of 9–26 carbons, there are still totally 324 possible species. Any one of these 324 molecular species may constitute a lipid component in the highly complex structure of biological membranes. Clearly, our current knowledge about the physical properties of saturated diacylphosphatidylcholines is far from complete. Among the various physical properties associated with fully hydrated phosphatidylcholines, the phase transition temperature,  $T_m$ , is the one that can be most accurately determined by high-resolution DSC. The prospect of trying to identify all of the unknown values of  $T_m$  seems daunting, based on the numerous organic syntheses and the time-consuming DSC experiments that are required. Consequently, it seems that other avenue must be explored to yield the  $T_m$  values of saturated diacylphosphatidylcholines. Indeed, there have been numerous recent studies on the prediction of the phase transition temperatures for these molecular species [6,10,20,21]. Although these predictions are highly successful, all of them are restricted to identical or mixed-chain phosphatidylcholines which, in excess water, undergo the partially interdigitated gel  $\rightarrow$  liquid-crystalline phase transition. In this study, extensive DSC experiments have been carried out to measure the  $T_m$  values for 52 molecular species of phosphatidylcholines which are highly asymmetrical with  $\Delta C/CL$  values in the range of 0.43 to 0.63. Based on these DSC results, empirical equations are derived to predict the  $T_m$  values for 81 molecular species of highly asymmetric phosphatidylcholines with  $\Delta C/CL$  values in the range of 0.43 to 0.63, which, in excess water, presumably would undergo the mixed interdigitated gel  $\rightarrow$  liquid-crystalline phase transition upon heating. Hence, the prediction of  $T_m$  values is now extended for the first time to include these highly asymmetrical species. Although the analysis of the DSC data described herein is not straight forward as that for less asymmetric molecular species as presented earlier [6], the following conclusions can be drawn from the present investigation.

(1) Based on the molecular packing model for the mixed interdigitated bilayer, it is suggested that the apparent chain length of the *sn*-2 acyl chain of mixed-chain phosphatidylcholines in the gel state in short-

ened by  $\sim 1.35$  C-C bond lengths due to the chain bend near the glycerol backbone region.

(2) For highly asymmetrical mixed-chain phosphatidylcholines which undergo the mixed interdigitated gel  $\rightarrow$  liquid-crystalline phase transition, the transition temperature,  $T_m$ , is a linear function of  $(\Delta C)^{-1}$  at a constant value of  $\delta$ .

(3) Based on the linear relationship between  $T_m$  and  $(\Delta C)^{-1}$  at the constant values of  $\delta$ , empirical equations can be derived to predict the  $T_m$  values for all highly asymmetrical mixed-chain phosphatidylcholines which, in excess water, would undergo the mixed interdigitated gel  $\rightarrow$  liquid-crystalline phase transition upon heating, and the predicted values are tabulated in Table II.

(4) The predicted  $T_m$  values can be regarded as reliable, since the comparison between the experimental and predicted values is excellent in all cases.

(5) Finally, it should be mentioned that the approach adapted here to predict the  $T_m$  value is empirical; however, it may form a basis for future theoretical studies. Moreover, this empirical approach is based on the molecular packing model of mixed interdigitation for fully hydrated asymmetric phosphatidylcholines (Fig. 1).

## Acknowledgments

This research was supported, in part, by U.S. Public Health Service Grant GM-17452 from the National Institute of General Medical Sciences, National Institutes of Health, Department of Health and Human Services. We appreciate greatly the contributions of Dr. Mantripragada B. Sankaram and Cheng-qui Zhang for their help in applying the various computer programs to the three-dimensional figures.

## References

- Huang, C. (1990) *Klin. Wochenschr.* 68, 149–165.
- Lin, H.-n., Wang, Z.-q. and Huang C. (1990) *Biochemistry* 29, 7063–7072.
- Lin, H.-n., Wang, Z.-q. and Huang, C. (1991) *Biochim. Biophys. Acta* 1067, 17–28.
- Bultmann, T., Lin, H.-n., Wang, Z.-q. and Huang, C. (1991) *Biochemistry* 30, 7194–7202.
- Mason, J.T., Huang, C. and Biltonen, R.L. (1981) *Biochemistry* 20, 6086–6092.
- Huang, C. (1991) *Biochemistry* 30, 26–30.
- Nagle, J.F. and Wilkinson, D.A. (1978) *Biophys. J.* 23, 159–175.
- Mason, J.T. and Huang, C. (1981) *Lipids* 16, 604–608.
- Small, D.M. (1986) in *Physical Chemistry of Lipids from Alkanes to Phospholipids*, pp. 475–522, Plenum Press, New York.
- Marsh, D. (1991) *Biochim. Biophys. Acta* 1062, 1–6.
- McIntosh, T.J., Simon, S.A., Ellington, J.C. and Porter, N.A. (1984) *Biochemistry* 23, 4038–4044.
- Hui, S.W., Mason, J.T. and Huang, C. (1984) *Biochemistry* 23, 5570–5577.
- Mattai, J., Sripada, P.K. and Shipley, G.G. (1987) *Biochemistry* 26, 3287–3297.

- 14 Yeagle, P. (1987) in *The Membranes of Cells*, pp. 22–61, Academic Press, New York.
- 15 Zaccai, G., Buildt, G., Seelig, A. and Seelig, J. (1979) *J. Mol. Biol.* 134, 693–706.
- 16 Huang, C., Mason, J.T. and Levin, I.W. (1983) *Biochemistry* 22, 2775–2780.
- 17 Shah, J., Sripada, P.K. and Shipley, G.G. (1990) *Biochemistry* 29, 4254–4262.
- 18 Huang, C. and Mason, J.T. (1986) *Biochim. Biophys. Acta* 864, 423–470.
- 19 Xu, H. and Huang, C. (1987) *Biochemistry* 26, 1036–1043.
- 20 Marsh, D. (1992) *Biophys. J.* 61, 1036–1040.
- 21 Cevc, G. (1991) *Biochemistry* 30, 7186–7193.